




Research Article

Optimization of welding parameters on pores migration in Laser-GMAW of 5083 aluminum alloy based on response surface methodology

Xiangru Ji^{1,2}  · Xueming Hua^{1,2} · Chen Shen^{1,2} · Ye Huang^{1,2} · Yuelong Zhang^{1,2} · Yan Cai^{1,2}

© Springer Nature Switzerland AG 2019

Abstract

The mathematical model to reveal the relationship between process parameters and pores migration distance of 5083 aluminum alloy Laser-GMAW was established based on the center composed design of response surface methodology. Three of the welding parameters were chosen as the factors: The welding current, welding speed, and the laser-arc distance. The distance between pores and weld bottom was calculated as the response value. The analysis of variance was used to test the significance of the model. According to the result of experiments, the low welding speed and high current were beneficial to decrease the solidification rate of the molten pool, the pores could overflow from the weld in time. When welding speed is increasing, it is necessary to appropriately increase the welding current and the Laser-arc distance, the volume of the molten pool would be expanded, pores were difficult to be caught by solidifying wall. The optimized parameters of the 30 mm aluminum alloy Laser-MIG hybrid welding were calculated based on the established model. The maximum pores migration distance can be obtained in 135 A/0.6 m/min/1.22 mm (welding current/welding speed/laser-arc distance).

Keywords Laser-arc welding · Pores migration · Response surface methodology

1 Introduction

The molten aluminum alloy has a small viscosity. During the Laser-GMAW of aluminum alloys, the keyhole is unstable, It easily collapses to cause pores-defects. Katayama [1] found that the high welding current is conducive to reduce the pores-defects, but further increasing the thickness of the workpiece (more than 4 mm), the pores-defects were still difficult to control. Marsunawa [2] used an X-ray high-speed imaging system to observe the keyhole stability and molten pool behavior during laser welding. They found the keyhole collapsing is a major factor of the pores generation, and Zhao [3] got a similar conclusion with him. Zhang et al.

[4] studied the relationship between the molten pool characteristics and the porosity of 6082 aluminum alloy in Laser hybrid welding. He pointed out that arc could expand the volume of the molten pool, and the larger volume of the molten pool, the easier escaping for the pores migration. However, most researchers used the workpieces thickness less than 8 mm, And there is less study on optimizing process parameters of the large-thickness aluminum alloy (more than 8 mm) in the Laser-GMAW. Haboudou [5] pointed out that the content of hydrogen and the content of Mg/Zn alloy are important factors leading to the collapsing of the keyhole. Zhang [6] believed that Laser-CMT hybrid welding can improve the stability of the laser welding and reduce

✉ Xueming Hua, xmhua@sjtu.edu.cn; Xiangru Ji, 13284502684@163.com; Chen Shen, cshen486@sjtu.edu.cn; Ye Huang, 645683578@qq.com; Yuelong Zhang, zhangyl@sjtu.edu.cn; Yan Cai, ycai@sjtu.edu.cn | ¹Shanghai Key Laboratory of Materials Laser Processing and Modification, School of Materials Science and Engineering, Shanghai Jiao Tong University, 800 Dongchuan Road, Shanghai 200240, People's Republic of China. ²Collaborative Innovation Centre for Advanced Ship and Deep-Sea Exploration, Shanghai 200240, People's Republic of China.



SN Applied Sciences (2019) 1:1161 | <https://doi.org/10.1007/s42452-019-1155-3>

Received: 1 July 2019 / Accepted: 23 August 2019 / Published online: 5 September 2019

the porosity in the weld. Ola and Doern [7] pointed out that the laser-arc distance could affect the pores defects. Nielsen [8] believed that laser hybrid welding was suitable for thick workpieces welding, compared with Laser welding, it has lower requirements for welding assemblage. Bunaziv [9] found that the addition of helium gas can effectively reduce the pores defects, but it has no obvious effect on the welding stability. However, it is difficult to completely solve the pores defects in aluminum alloy laser welding. It is necessary to optimize the process parameters of the aluminum alloy Laser-GMAW, and the pores in the aluminum alloy welding can float out of the weld as much as possible.

There are interactions between various parameters, so it is not possible to design a single factor test to establish the mathematical model. Response surface methodology (RSM) can effectively evaluate the interaction between various parameters. Many models were built to optimize the welding parameters in the welding area by using RSM. Cai [10] used RSM to optimize the ternary shielding gas composition in the tandem narrow gap welding of Q235, When the shielding gas composition was at 10% CO₂, 79% Ar and 11% He, the welding solidifying wall penetration was increased, and the solidifying wall defects was avoided. Karthikeyan and Balasubramanian [11] used RSM to predict the optimized friction spot welding process parameters for joining AA2024 aluminum alloy. Olabi [12] used the response surface methodology to optimize the CO₂ laser welding process parameters of dissimilar materials. Benyounis [13] used RSM to optimize the laser-welding parameters of medium carbon steel. Elatharasan and Kumar [14] used the Response Surface Method to optimize the process parameters of 6061 aluminum alloy friction stir welding, and they also established a model to reveal the relationship between the process parameters and the mechanical properties.

In this study, Based on the response surface methodology, A mathematical model was established to reveal the relationship between Laser-welding parameters and the pores migration distance. An optimized parameter was found, so the pores will overflow from the weld during the 5083 aluminum alloy thick workpiece Laser-GMAW. In our previous work, Welding current, welding speed and Laser-arc distance were chosen as the factors. Welding current ranges in 100–150 A, When the welding current is higher than 150 A or lower than 100 A, the welding is unstable. Welding speed ranges of 0.50–1.00 m/min, and the distance between the laser and arc ranges of 0.00–6.00 mm.

2 Experimental set-ups

The experimental system was sketched in Fig. 1. A Fronius TransPuls Synergic5000 GMAW power source and an IPG-YLS10000 Laser power source were used as the welding

power source. The laser power was set at 10 kW to ensure max penetration (over 15 mm). The diameter of laser spot is 0.6 mm, the focal length of the lens is 300 mm, and the defocus was set as 0 mm. The angle between Laser and vertical direction was set at 8°, and the angle between the arc gun and the workpiece was set to 60°. The laser leads the arc during the welding. The 30 mm 5083 aluminum alloy were chosen as the base metal. 5183 aluminum alloy wire was selected as the filler metal, the chemical composition of the base metal and welding wire is shown in Table 1. The pure Ar was chosen as the shielding gas. In order to avoid the pores escaping from the gap of weld bottom, the workpieces were welded without the groove.

The sections were cut off in the middle part of the weld, Five specimens were cut from each weld, there were 3–5 mm interval between each specimen. Both sections of the specimens were polished by sandpaper, the distance between the pores and the bottom of the weld was measured by polarizing microscope (Leica DM4000). The pores migration distances of five specimens were calculated and averaged to reduce the measurement error. The average value was given as the final response value.

In this study, three-factor center composed design (CCD) method was used to design the experiment, the steps of this experiment are as follows:

- Selecting variables and a range of variables.
- Designing test plans with software design-expert 7.0.
- Performing welding experiments according to test plan.
- Processing specimens, observing and recording experiment results.
- Entering the experimental results, and using software calculations to establish the fitting equations and models.

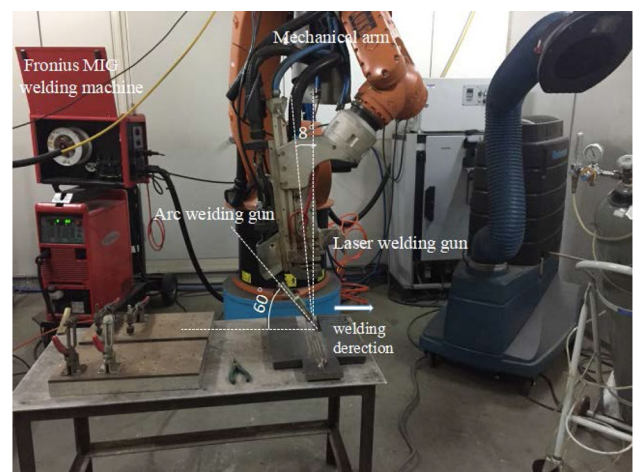


Fig. 1 Set up of experimental system

Table 1 Chemical composition of base metal and filler metal (wt%)

Element	Al	Si	Cu	Mg	Zn	Mn	Ti	Cr	Fe
Base metal	Bal.	≤0.40	≤0.10	4.0–4.9	≤0.25	0.40–1.0	≤0.15	0.05–0.25	0.00–0.40
Filler metal	Bal.	0.40	0.10	4.3–5.2	0.25	0.50–1.00	0.05–0.20	0.05–0.25	0.40

- (f) Testing the accuracy of the fitted model.
- (g) Analysis of results.

Based on the mathematical model, an optimized parameter was given to get the largest pores migration distance, then compare the fact-value and theoretical value.

3 Create a fitting model

The response surface methodology (RSM) is a kind of statistical experimental design. The method is used to establish a continuous variable surface model to evaluate the interaction of factors, and figure out the relationship between the factors and the response values. In this experiment, center composed design (CCD) was used to design the experiment. CCD adds a center point and the axial points on the basis of the orthogonal design of regression, the experimental matrix has rotation and orthogonality. Taking a two-factor CCD experiment as an example, the CCD setup process is briefly introduced. As shown in Fig. 2, they are two factors in the experiment, so a flat rectangular coordinate system is established. There are three types of experimental points in this coordinate system: full-factor test points $(\pm 1, \pm 1)$, test points on the factor axis $(0, \pm \alpha)/(\pm \alpha, 0)$, and central test points $(0, 0)$. In order to ensure the rotation of the test parameter matrix, the test points with the same distance from the center point have the same variance.

$$\alpha = (2^k)^{1/4} \tag{1}$$

The maximum and the minimum of input variables are coded as $\pm \alpha$, the upper level and the lower level are encoded as ± 1 , and the center value is coded as 0. The relationship between the actual value and the coded value is as follows:

$$X_i = \frac{\alpha * (2X - (X_{max} + X_{min}))}{X_{max} - X_{min}} \tag{2}$$

In this formula: X_i —coded value of Variable X; X_{max} —The maximum value that the variable X can reach; X_{min} —The minimum value that the variable X can reach.

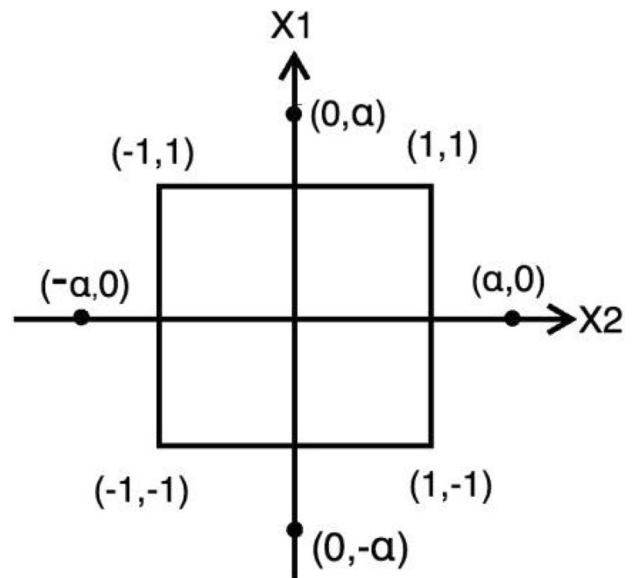


Fig. 2 Design schematic of CCD

In this study, the welding current (I), welding speed (V) and Laser-arc distance (L) were selected as the experiment factors. When the aluminum alloy is laser-welded, Huang [15] found the keyhole collapsing often occur at the bottom of the weld. The distance between the weld bottom to the pores can be considered as the pores migration distance. The distance from the pores to the bottom of the weld (S) is chosen as the response value to reveal the parameters' effect on the pores migration.

Table 2 shows the correspondence between the encoded values and the actual values of the variables.

Table 3 shows the experimental plan. Welding current ranged in the 100–150 A, Welding speed ranged of 0.50–1.00 m/min, and the Laser-arc distance ranged of 0.00–6.00 mm.

Finish the experiments based on the designed plan, five specimens were cut at the middle part of the weld, each specimen has two sections, measured the pores migration distance of each section, the results were calculated and averaged as the final response value, Fig. 3 shows the welding process during the experiment. Figure 4 shows the weld cross-section. The final results are given in Table 3. The fitting formulas for various process parameters on the pores behavior are obtained as flow:

Table 2 The correspondence between the encoded values and the actual values

Factors	Unit	Coded value				
		-1	1	0	-1.68	1.68
I	A	110	140	125	100	150
V	m/min	0.60	0.90	0.75	0.50	1.00
L	mm	1.22	4.78	3.00	0.00	6.00

Table 3 the experimental protocol

Run	Current	Welding speed	Laser arc distance	The distance of pores floating (mm)
1	0	0	0	13.524
2	0	0	0	13.300
3	1	-1	1	16.400
4	0	0	0	15.090
5	0	0	0	13.415
6	1	1	1	16.880
7	-1	1	-1	11.120
8	0	-1.68	0	17.020
9	1	1	-1	12.270
10	-1	1	1	10.650
11	-1.68	0	0	6.930
12	-1	-1	1	10.740
13	0	0	1.68	14.020
14	-1	-1	-1	16.800
15	0	0	-1.68	13.150
16	0	1.68	0	13.640
17	0	0	0	13.900
18	0	0	0	11.140
19	1.68	0	0	12.763
20	1	-1	-1	18.045

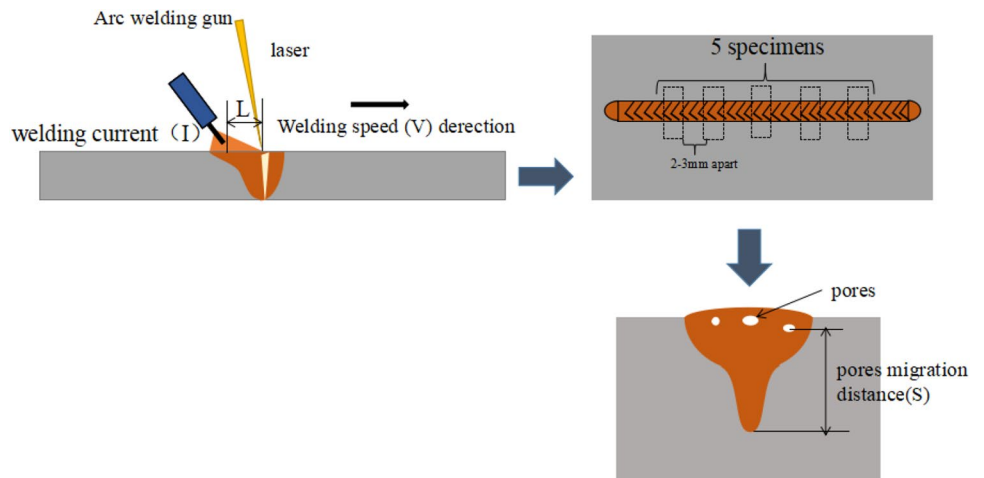
$$S = 3.41381 + 0.94870 \times I - 100.89797 \times V - 10.72069 \times L + 0.026870 \times I \times V + 0.044760 \times I \times L + 5.58379 \times L \times V - 0.00393788 \times I^2 + 48.35821 \times V^2 + 0.14193 \times L^2$$

In this formulas: S—the distance of pores floating; I—the welding current; V—the welding speed; L—the distance of laser and arc.

This mathematical model was tested by ANOVA technique, the test results are shown in Table 4. The probability of F(Prob > F value of model) is 0.0002 (less than 0.05), it means that the fitting model is significant. The probability of a lack of fit (P value is larger than the F value) is 0.3264 (more than 0.05), which means that the lack of fit is not significant. The mathematical model is convergent.

Figure 5 shows the predicted residual distribution, the residual values are scattered on both sides of the predicted line, which means the residuals were random, the model was accurate. Figure 6 shows the forecast and actual values distribution, the actual values are distributed on both sides of the predicted line, the actual values were closed to the predicted values. Figure 7 shows the residual values normal distribution, as can be seen from Fig. 7, the distribution of residual values basically meets the normal distribution, and the fitting result is accurate.

Fig. 3 Welding process during the experiment



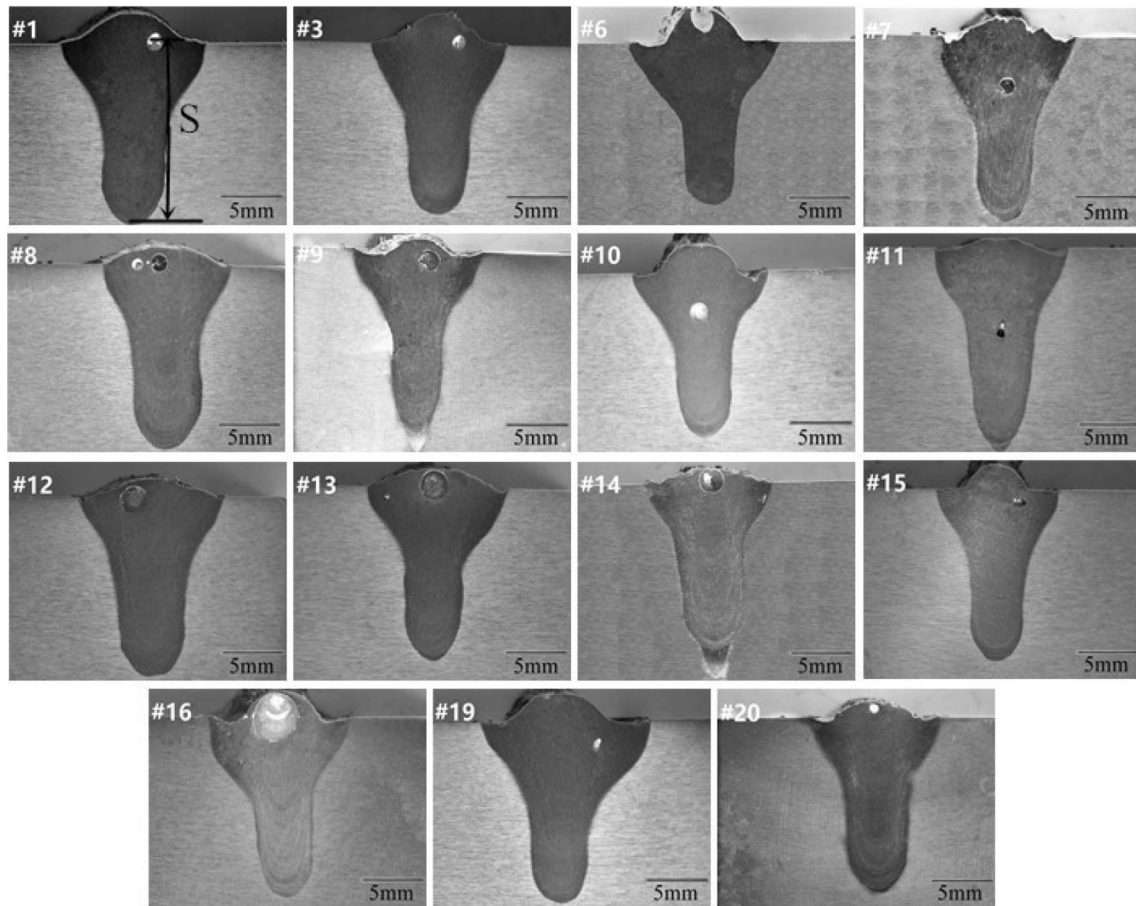


Fig. 4 The weld cross-section

Table 4 the F-test data of the fitted equations

Source	Sum of squares	Df	Mean square	F value	P value	Prob > F
Model	125.30	9	13.92	12.43	0.0002	Significant
I	42.51	1	42.51	37.95	0.0001	
V	20.54	1	20.54	18.34	0.0016	
L	0.32	1	0.32	0.29	0.6028	
I*V	0.028	1	0.028	0.025	0.8771	
I*L	11.27	1	11.27	10.06	0.0100	
V*L	17.54	1	17.54	15.66	0.0027	
I*I	10.91	1	10.91	9.74	0.0109	
V*V	16.46	1	16.46	14.69	0.0033	
L*L	2.94	1	2.94	2.62	0.1363	
Residual	11.20	10	1.12	–	–	
Lack of fit	6.77	5	1.35	1.53	0.3264	Not significant
Pure error	4.43	5	0.89	–	–	
Cor total	136.50	19	–	–	–	

4 Effect of process parameters on pores migration distance

Based on the mathematical model, the parameters’ effects on the pores migration distance were analyzed by the

Design Expert 8.0. The interaction of each two parameters were given in the 3D-Response surface. When the other parameter ranged from low level to high level, The 3D-Response surface also changed.

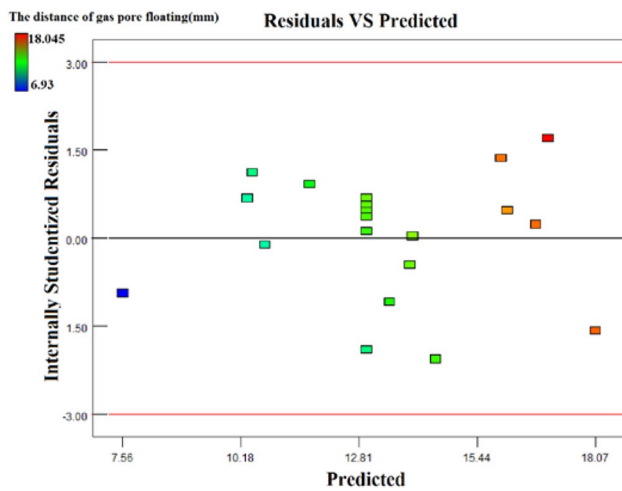


Fig. 5 Predicted residual distribution

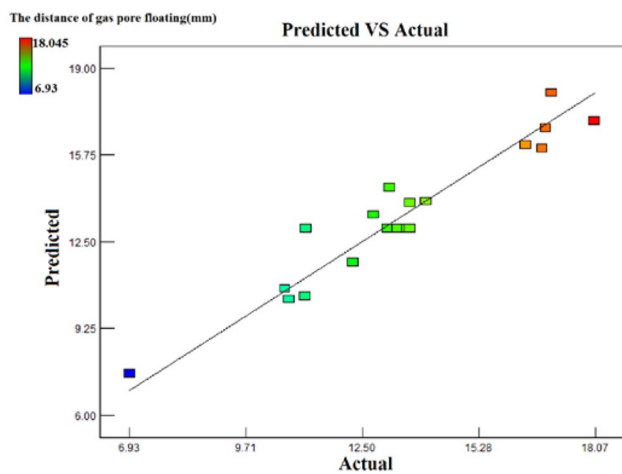


Fig. 6 Forecast and actual value distribution

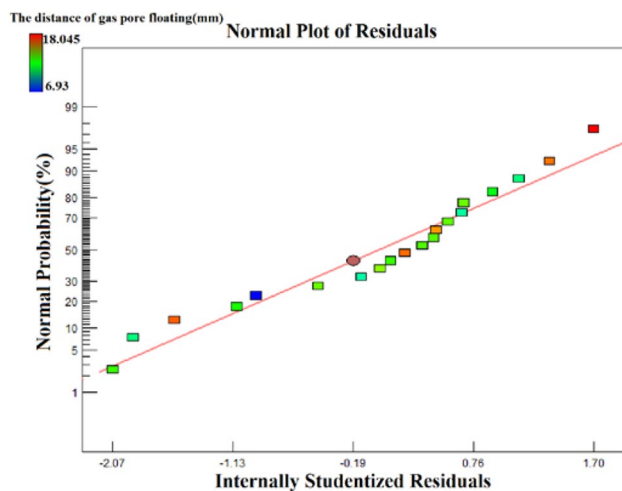


Fig. 7 Residual values normal distribution

4.1 Effect of welding speed and laser-arc distance on pores migration

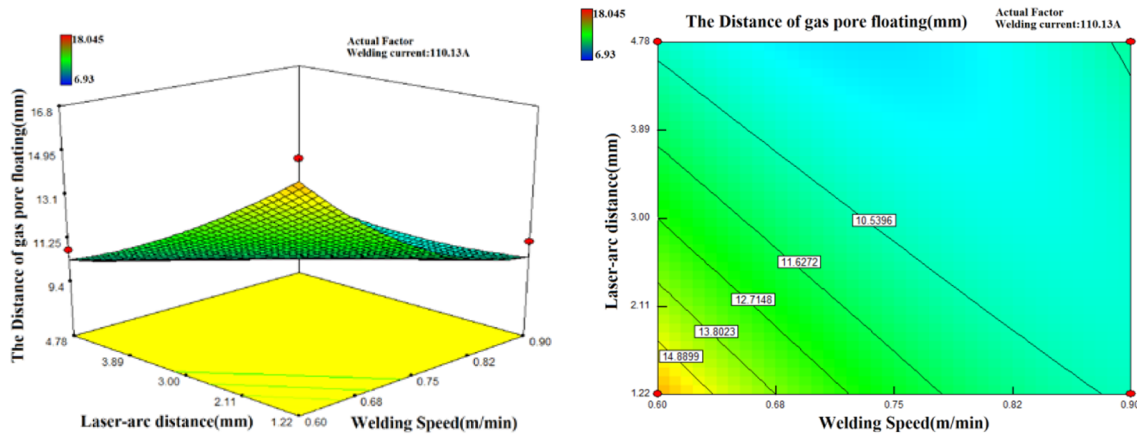
Effect of welding speed and laser-arc distance on pores migration were summarized. The response surfaces are presented in Fig. 8. When the welding current was at the low level (110 A), A high pores migration distance (around 15 mm) can be obtained when the welding speed is below 0.60 m/min, and the Laser-arc distance is below 1.5 mm. The current increased to 125 A, the response surface was folded along the diagonal. The pores migration distance was more than 15 mm when the welding speed is below 0.65 m/min and the Laser-arc distance is below 2.11 mm. Until the welding current increased to 139 A, The response surface was up to a higher position, more than 50% response surface was above 14 mm.

4.2 Effect of welding current and laser-arc distance on pores migration

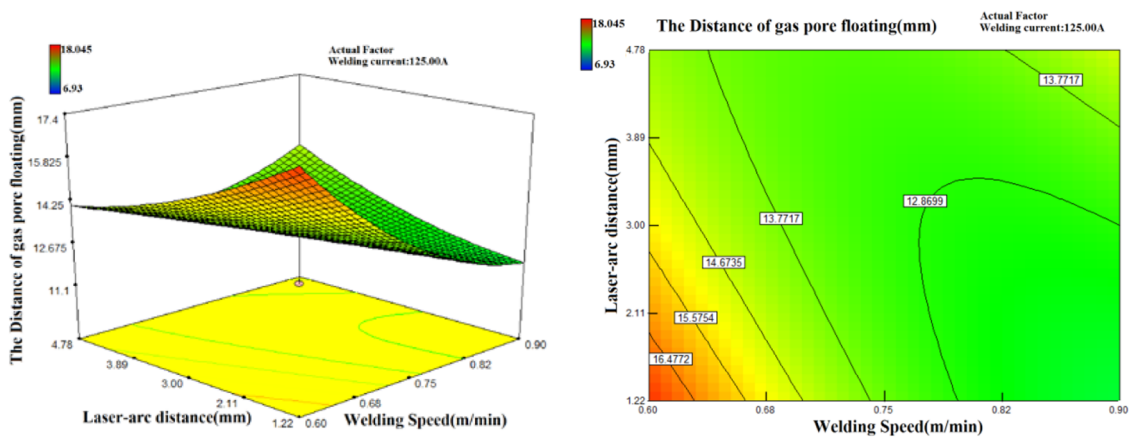
The effect of the welding current and Laser-arc distance on pores migration were shown in Fig. 9. When the welding speed is 0.6 m/min, pores migration distance was over 16 mm when the Laser-arc distance was set as 1.22 mm. When the welding speed gradually increased to 0.75 m/min, the entire surface moves downward, the maximum pores migration distance does not exceed 15.4 mm. And the contour line gradually becomes the vertical direction, which means the welding current was the main factor of pores migration. When the welding speed is increased to 0.9 m/min, part of the surface was up to the high position, the other part still remains in the low position. Only the welding current is over 130 A, and the Laser-arc distance is more than 4 mm, a large pores migration distance could be obtained. When the welding speed is at a low level, the molten pool cooling rate is slow, the pores have enough time to overflow from the molten pool, so the welding parameters window is relatively large. As the welding speed increases, the weld cools faster. The welding current and laser-arc distance should be increased to enlarge the molten pool volume and reduce the cooling rate, so the pores can escape from the molten pool.

4.3 Effect of welding speed and welding current on pores migration

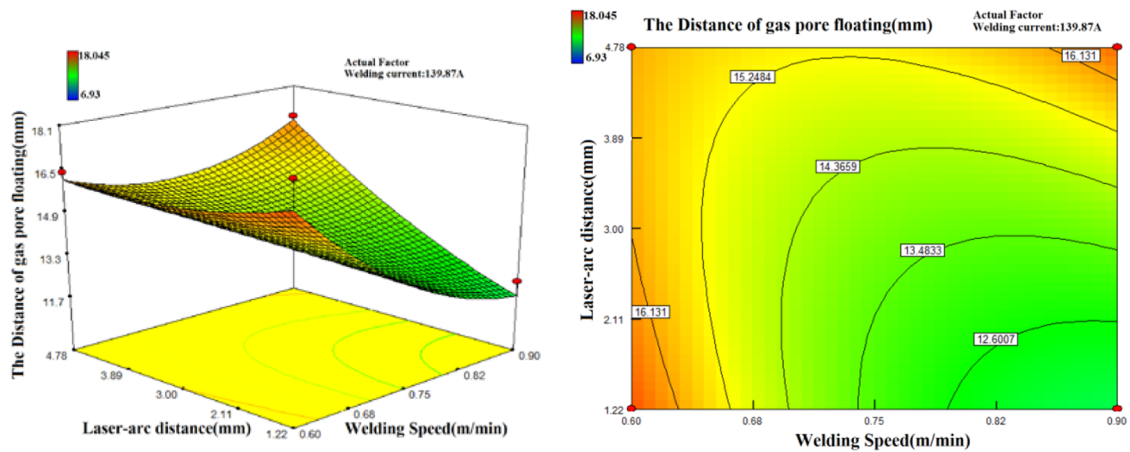
Figure 10 shows the effect of welding current and welding speed on pores migration. When the laser-arc distance reached 1.22 mm, the contour lines were at the horizontal position, welding speed is the main factor of pores migration, a large pores migration distance can be obtained



(a) Low welding current (110A), response surface map (left) and contour map (right)

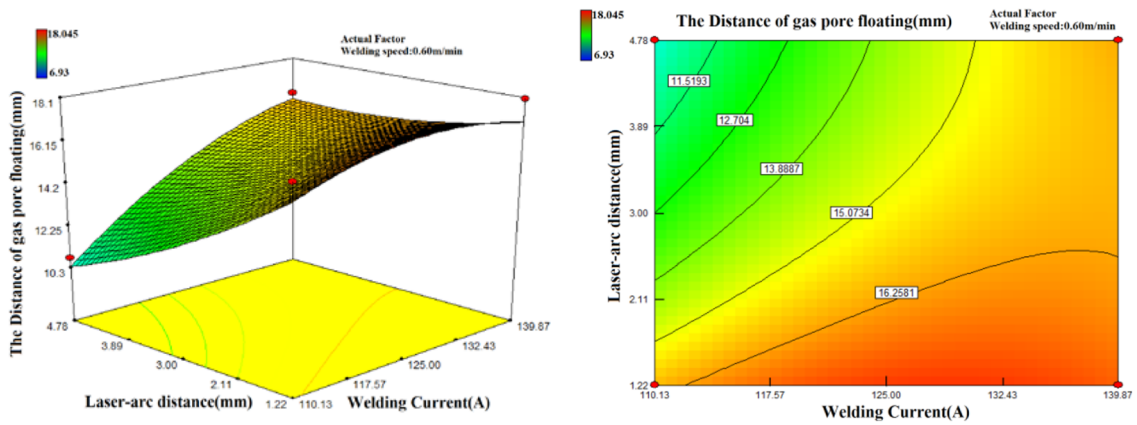


(b) Middle welding current (125A), response surface map (left) and contour map (right)

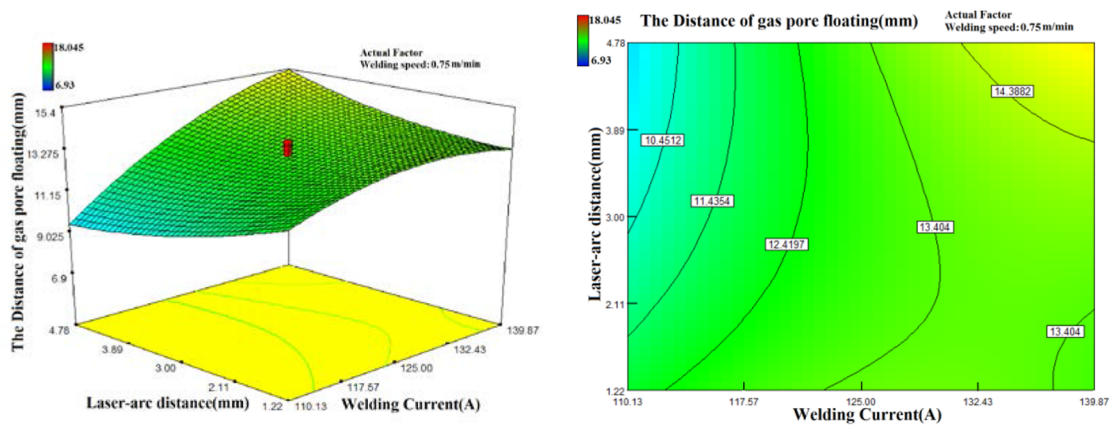


(c) High welding current (140A), response surface map (left) and contour map (right)

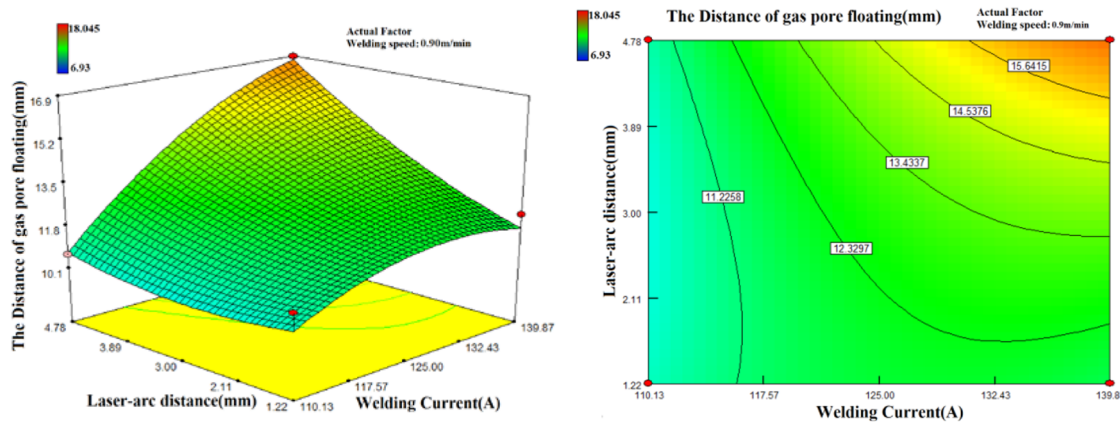
Fig. 8 In different welding current, response surface map and contour map



(a) Low welding speed (0.6m/min), response surface map (left) and contour map (right)



(b) Middle welding speed (0.75m/min), response surface map (left) and contour map (right)

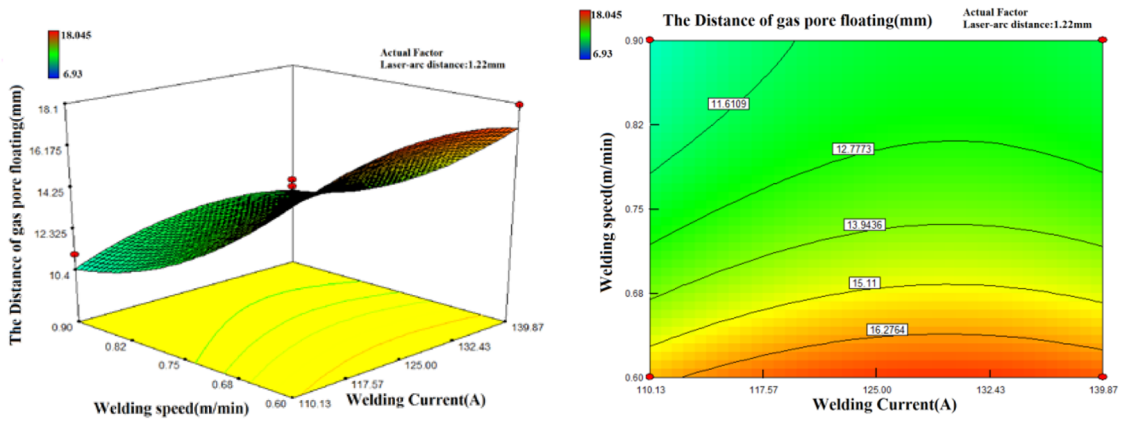


(c) High welding speed (0.9m/min), response surface map (left) and contour map (right)

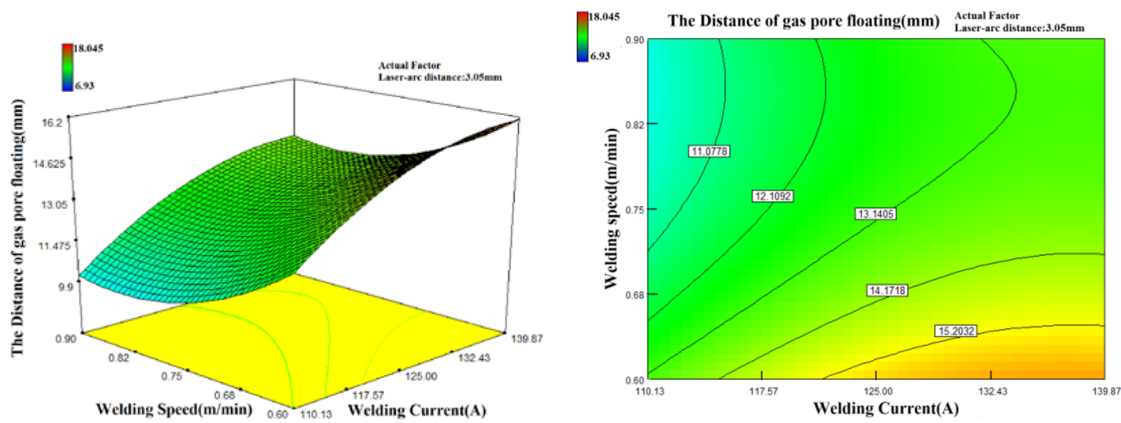
Fig. 9 In different welding current, 3D-Response surface and contour map

when the welding speed was lower than 0.65 m/min. As the laser-arc distance increased to 3.05 mm, the contour lines gradually changed from horizontal to vertical,

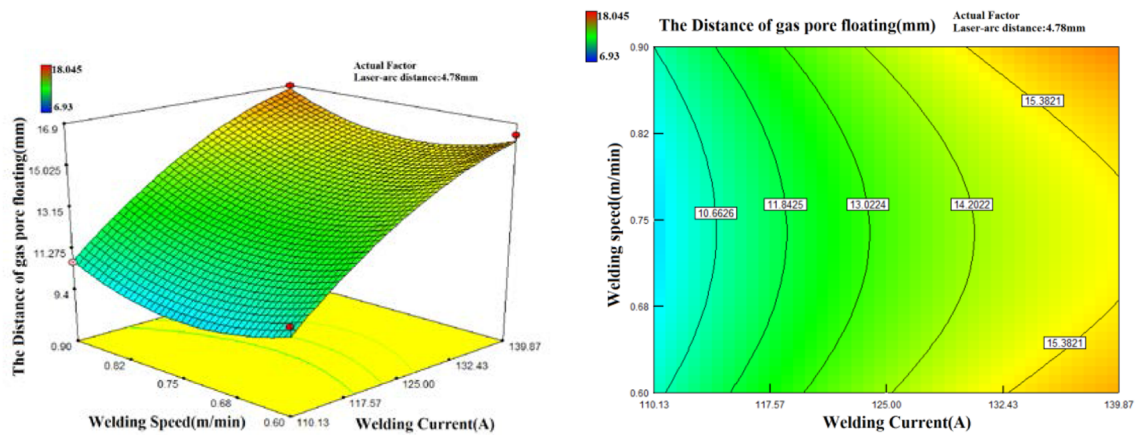
the response surface moved to a lower position. When the laser-arc distance increased to 4.78 mm, the welding



(a) Low laser-arc distance (1.22mm), response surface map (left) and contour map (right)



(b) Middle laser-arc distance (3.05mm), response surface map (left) and contour map (right)



(c) High laser-arc distance (4.78mm), response surface map (left) and contour map (right)

Fig. 10 In different welding current, response surface map and contour map

current is the main factor on pores migration, and the contours become vertical.

In a low laser-arc distance, the volume of molten pool is small, the molten pool solidification rate is mainly determined by the laser power and welding speed. Laser power has been selected as 10 kW to ensure the max penetration, the welding speed becomes the main factor of solidification rate. When the Laser-arc distance increased, the volume of the molten pool increased, and the shape of the molten pool changes. The cooperation between the arc and laser decreased due to the large laser-arc distance. The welding current determines the volume and the cooling rate of the molten pool.

4.4 Result analysis

A large pores migration could be obtained at the low welding speed, the high welding current, and small laser-arc distance. When the welding speed increased, it is necessary to increase the welding current and the laser-arc distance at the same time. Figure 11 shows how the parameters influence the pores migration. The pores migration was decided by the cooling rate and the shape of the molten pool. A large volume of molten pool and low cooling rate are beneficial to pores escaping during

the welding. As is shown in Fig. 11, at a slow welding speed, it would take a long time to curdle the weld, the pores had enough time to overflow from the molten pool, and the laser-arc distance has no obvious effect on pores migration.

The size of the arc crater of the weld under some typical parameters was measured and recorded in Table 5. As shown in Fig. 11, when the welding speed is at a low level, the molten pool cooling rate is slow. In this case, the pores will have enough time to escape from the molten pool. No. 20 and No. 3 weld are the typical weld of the low welding speed model. No. 20 weld has a very small laser-arc distance (1.22 mm), and No. 3 weld has a large laser-arc distance (4.78 mm), but both of them have relatively high pores migration distances. When the welding speed is relatively large, the solidification speed of the molten pool is accelerated. When the laser-arc distance is at a low level, the volume of the molten pool is smaller, and the pores are more likely to be captured by the sidewall of the molten pool. The No. 9 weld is the typical weld of a high welding speed and a small laser-arc distance model, and the pores was captured by the side wall of molten pool. As can be seen from Table 5, the crater size of No. 9 weld is similar to No. 20, but it is obviously smaller than No. 6 and No. 3 welds, which proves that the molten pool volume of weld No.

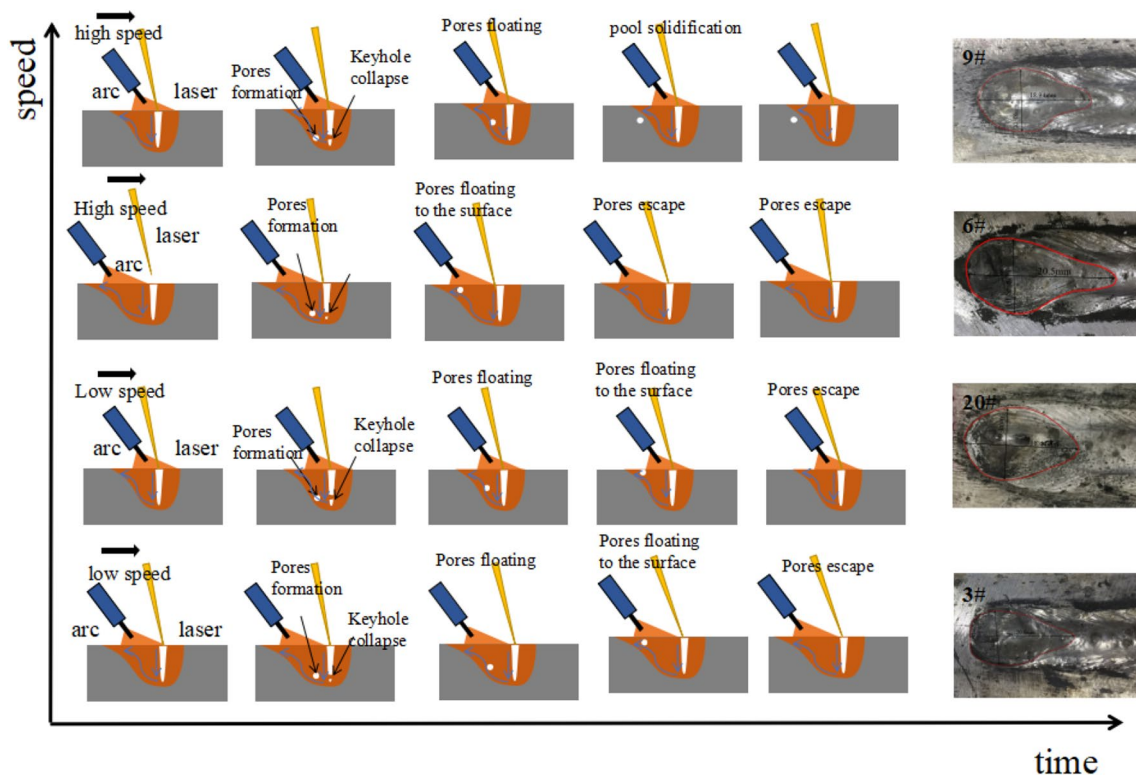
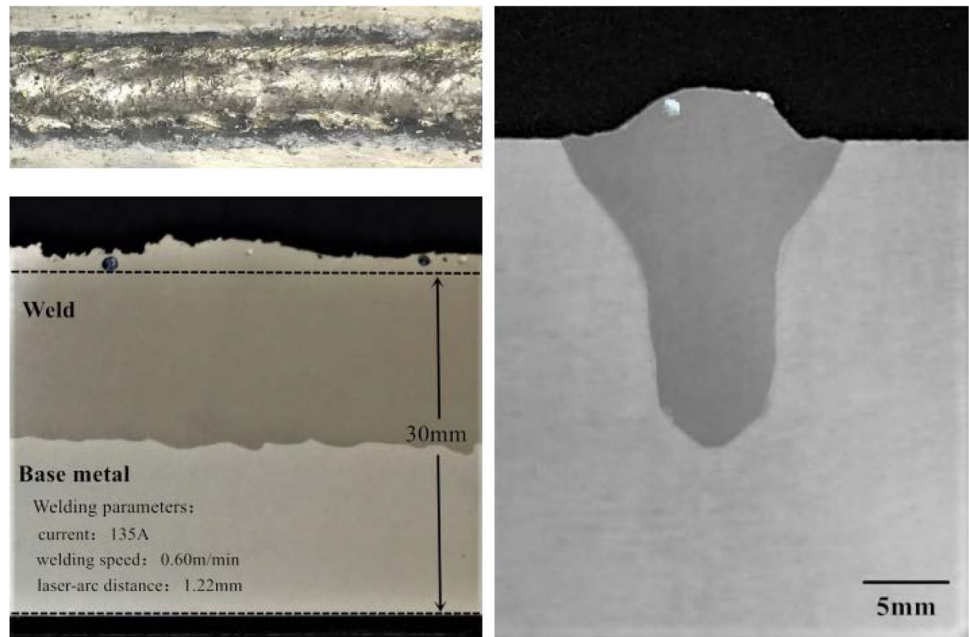


Fig. 11 Schematic diagram of pores migration and morphology of arc pits in welds

Table 5 Welded arc pit size

Number	Current (A)	Welding speed (m/min)	Laser-arc distance (mm)	Crater pit lateral length (mm)	Crater pit longitudinal length (mm)	Pores migration distance (mm)
9	140	0.90	1.22	18.94	10.18	12.27
6	140	0.90	4.78	20.50	10.60	16.88
20	140	0.60	1.22	18.44	10.40	18.05
3	140	0.60	4.78	20.60	11.70	16.40

Fig. 12 The weld surface (left) and the longitudinal section of the weld (right)



9 is smaller than No. 6 and No. 20. On the other hand, when the laser-arc distance is at a high level, the volume of the molten pool increases, so the pores is much difficult to be captured by the side wall. The No. 6 weld is the typical weld of high weld speed and high laser-arc distance model. The crater pit size of No. 6 weld larger than the No. 9 and No. 20, but the pores migration distance of No. 6 is more than 16 mm.

4.5 Optimized process parameters

The purpose of this experiment is to find an optimized parameter so that pores can overflow from the weld. The boundary condition was selected as the max pores migration distance, after software calculation, the optimal parameters are as follows: welding current is at 135 A, welding speed is at 0.6 m/min, and the laser-arc distance is at 1.22 mm. The weld surface and the section are shown in Fig. 12. It can be seen from the

Table 6 Predicted and actual values of the pores migration distance

	Welding current (A)	Welding speed (m/min)	Laser-arc distance (mm)	Pores migration distance (mm)	Error (%)
Predictive value	135	0.6	1.22	17.33	–
Actual value	135	0.6	1.22	16.70	3.6

picture that the pores basically overflow from the weld to the remaining high part. The predicted value and actual value of the pores migration distance are given in Table 5. The error between the predicted value and the actual value is less than 5%, the mathematical model is correct (Table 6).

5 Conclusions

This article mainly about the mathematical model established based on the RSM to reveal the relationship between the parameters and the pores migration. The results are as follows:

1. Based on the CCD method of response surface methodology, a model was established to figure out the effects of welding current, welding speed, and laser-arc distance on the distance of pores migration during the laser hybrid welding of 30 mm 5083 aluminum alloy.
2. When the welding speed is at a low level, the larger welding current is benefit for pores migration, but the laser-arc distance has no obvious effect on pores escaping, the molten pool cool rate is slow, and larger pores migration distance can be obtained. When the welding speed is at a high level, the molten pool cooling rate is faster, and it is necessary to increase the welding speed and the Laser-arc distance at the same time to increase the volume of the molten pool, so the pores can not be captured by the side wall of molten pool.
3. Based on the mathematical model, the optimal parameters can be obtain: 135 A/0.6 m/min/1.22 mm (welding current/welding speed/laser-arc distance). The error between predict value and actual value is less than 5%, the mathematical model based on the CCD is correct.

Acknowledgements I would like to declare on behalf of my co-authors that the work described was original research that has not been published previously, and not under consideration for publication elsewhere, in whole or in part. All the authors listed have approved the manuscript that is enclosed. This study has no founding support.

Compliance with ethical standards

Conflict of interest No conflict of interest exists in the submission of this manuscript, and manuscript is approved by all authors for publication.

References

1. Katayama S, Uchiumi S, Mizutani M, Wang J, Fujii K (2007) Penetration and porosity prevention mechanism in YAG laser-MIG hybrid welding. *Weld Int* 21:25–31
2. Matsunawa A, Kim J-D, Seto N, Mizutani M, Katayama S (1988) Dynamics of keyhole and molten pool in laser welding. *J Laser Appl* 10:247–254
3. Zhao H, White DR, DebRoy T (2013) Current issues and problems in laser welding of automotive aluminium alloys. *Int Mater Rev* 44:238–266
4. Zhang C, Gao M, Wang D, Yin J, Zeng X (2017) Relationship between pool characteristic and weld porosity in laser arc hybrid welding of AA6082 aluminum alloy. *J Mater Process Technol* 240:217–222
5. Haboudou A, Peyre P, Vannes AB, Peix G (2003) Reduction of porosity content generated during Nd:YAG laser welding of A356 and AA5083 aluminium alloys. *Mater Sci Eng A* 363:40–52
6. Zhang C, Gao M, Zeng X (2016) Effect of microstructural characteristics on high cycle fatigue properties of laser-arc hybrid welded AA6082 aluminum alloy. *J Mater Process Technol* 231:479–487
7. Ola OT, Doern FE (2015) Keyhole-induced porosity in laser-arc hybrid welded aluminum. *Int J Adv Manuf Technol* 80:3–10
8. Nielsen SE (2015) High power laser hybrid welding—challenges and perspectives. *Phys Procedia* 78:24–34
9. Bunaziv I, Akselsen OM, Salminen A, Unt A (2016) Fiber laser-MIG hybrid welding of 5 mm 5083 aluminum alloy. *J Mater Process Technol* 233:107–114
10. Cai X, Fan C, Lin S, Ji X, Yang C (2017) Optimization of shielding gas composition in narrow gap GMA welding based on response surface methodology. *Int J Adv Manuf Technol* 95:2405–2412
11. Karthikeyan R, Balasubramanian V (2010) Predictions of the optimized friction stir spot welding process parameters for joining AA2024 aluminum alloy using RSM. *Int J Adv Manuf Technol* 51:173–183
12. Olabi AG, Alsinani FO, Alabdulkarim AA, Ruggiero A, Tricarico L, Benyounis KY (2013) Optimizing the CO₂ laser welding process for dissimilar materials. *Opt Lasers Eng* 51:832–839
13. Benyounis KY, Olabi AG, Hashmi MSJ (2005) Optimizing the laser-welded butt joints of medium carbon steel using RSM. *J Mater Process Technol* 164–165:986–989
14. Elatharasan G, Kumar VSS (2013) An experimental analysis and optimization of process parameter on friction stir welding of AA 6061-T6 aluminum alloy using RSM. *Procedia Eng* 64:1227–1234
15. Huang L, Hua X, Wu D, Fang L, Cai Y, Ye Y (2018) Effect of magnesium content on keyhole-induced porosity formation and distribution in aluminum alloys laser welding. *J Manuf Process* 33:43–53

Publisher's Note Springer Nature remains neutral with regard to jurisdictional claims in published maps and institutional affiliations.